Pramana – J. Phys. (2019) 93:66
https://doi.org/10.1007/s12043-019-1819-y

Numerical solution of nonlinear fractional Zakharov–Kuznetsov equation arising in ion-acoustic waves

AMIT PRAKASH[1],* and VIJAY VERMA[2]

[1]Department of Mathematics, National Institute of Technology, Kurukshetra 136 119, India
[2]Department of Mathematics, Pt. Chiranji Lal Sharma Govt. (PG) College, Karnal 132 001, India
*Corresponding author. E-mail: amitmath@nitkkr.ac.in; amitmath0185@gmail.com

MS received 10 January 2019; revised 8 April 2019; accepted 15 April 2019

Abstract. The main purpose of this work is to suggest an efficient hybrid computational technique, namely the q-homotopy analysis transform method (q-HATM) to find the solution of the nonlinear time-fractional Zakharov–Kuznetsov (FZK) equation in two dimensions. The uniqueness and convergence analysis of the nonlinear time-FZK equation is presented. The Laplace decomposition method (LDM) is also employed to get the approximate solution of the nonlinear FZK equation. We implemented these techniques on two numerical examples, plotted the solution and compared the absolute error with the variational iteration technique and homotopy perturbation transform technique to show the efficiency of these techniques.

Keywords. Zakharov–Kuznetsov equation; q-homotopy analysis transform method; Caputo fractional derivative; Laplace decomposition method.

PACS Nos 02.60.–Cb; 05.45.–a

1. Introduction

Numerous important models are being modelled in various significant areas like control, signal theory, mechanical, acoustics, fluid and in many other engineering sciences using fractional derivatives. In day-to-day life, we cannot imagine any model without fractional derivatives. There are many nonlinear models in this Universe and precisely we can say that it is almost impossible to solve nonlinear fractional models. So we have to find out the approximate solution to the nonlinear fractional models. There are many techniques such as the variational iteration method [1–5], homotopy perturbation method [6,7], homotopy analysis transform method (HATM) [8–11], new iterative Sumudu transform method [12], Adams–Bashforth–Moultan method [13], residual power series method [14], fractional natural decomposition method [15], modified extended direct algebraic method [16], fractional HATM [17], q-HATM [18,19], fractional variational iteration method [20–22] and many other methods which help us to find the approximate solution.

This article studies the merit of q-HATM to find the solution of the nonlinear time-fractional Zakharov–Kuznetsov (FZK) equation in two dimensions. The q-HATM is a smooth combination of two great methods, q-homotopy analysis method (HAM) and the Laplace transform, and gives solutions in the form of a convergent series in an easy way. El-Tawil and Huseen [23,24] proposed and cultivated q-HAM first for solving linear and nonlinear differential equations. This technique is an expansion of the embedding parameter $q \in [0, 1]$ which was studied by Liao [25–27] in HAM to $q \in [0, 1/n]$ that acts in q-HAM. The HAM is dependent on homotopy, a fundamental conviction in the topic of differential geometry and topology, which is implemented to find the solution of linear and nonlinear models arising in numerous fields of scientific area [28–32]. The HAM is combined with the Laplace transform to obtain an extremely operative method to study nonlinear problems of day-to-day life [33–35]. It is an eminent point that the combinations of semianalytical techniques with the Laplace transform provide less CPU time to investigate nonlinear problems describing engineering applications.

In the present paper, we study the ensuing nonlinear time-FZK equations (FZK(p, q, r)) of the type

$$D_t^{\beta} u + a(u^p)_x + b(u^q)_{xxx} + c(u^r)_{xyy} = 0, \qquad (1)$$

Published online: 31 July 2019

where $u = u(x, y, t)$, β is a parameter characterising the order of the time-fractional derivative $0 < \beta \leq 1$, where a, b and c are arbitrary constants, p, q and r are integers and p, q and $r \neq 0$ manage the behaviour of weakly nonlinear ion-acoustic waves in a plasma comprising cold ions and hot isothermal electrons in the presence of a uniform magnetic field [36,37]. This equation was first obtained for expressing weakly nonlinear ion-acoustic waves in strongly magnetised lossless plasma in two dimensions [38]. The FZK equations have been studied previously by using new iterative Sumudu transform method (NISTM) [12], variational iteration method (VIM) [39], homotopy perturbation method (HPM) [40] and homotopy perturbation transform method (HPTM) [41] with their limitations. The key motivation for writing this paper is to put up a reliable computational technique to examine nonlinear fractional differential equations because of their utilities in mathematical modelling of real-word problems in a more accurate and systematic manner [42–45]. In the present paper, we propose the q-HATM and the Laplace decomposition method (LDM) to find the solution of the FZK equations. The q-HATM is a joint form of the standard Laplace transform and q-HAM. The improvement of this method is its competency of joining two strong techniques for approximate analytical solutions of nonlinear equations. It is worth mentioning that the proposed approach is capable of reducing the volume of computational work compared to the classical schemes while still maintaining the high accuracy of the numerical results; the size reduction amounts to an improvement of the performance of the approach.

2. Basic definition of the Laplace transform and fractional calculus

DEFINITION 2.1

We can define the Laplace transform of a given function $g(t)$ as [46]

$$L[g(t)] = g(s) = \int_0^\infty \mathrm{e}^{-st} g(t)\mathrm{d}t.$$

DEFINITION 2.2

Laplace transform $L[g(t)]$ of the Caputo fractional derivative is defined as [46]

$$L[D_t^\beta g(t)] = s^\beta g(s) - \sum_{k=0}^{m-1} s^{(\beta-k-1)} f^{(k)}(0), \quad m-1 < \beta \leq m.$$

3. Basic idea of the q-HATM

In this section, we present the basic theory and solution procedure of the proposed technique. We take a general fractional nonlinear non-homogeneous partial differential equation of the form

$$D_t^\alpha u(x,t) + Ru(x,t) + Nu(x,t) = g(x,t),$$
$$n-1 < \alpha \leq n, \tag{2}$$

where $D_t^\alpha u(x,t)$ represents the fractional derivative of the function $u(x,t)$ in terms of Caputo, R indicates the linear differential operator, N represents the general nonlinear differential operator and $g(x,t)$ is the source term. By applying Laplace transform operator on both sides of eq. (2), we get

$$L\left[D_t^\alpha u(x,t)\right] + L[Ru(x,t)] + L[Nu(x,t)] = L[g(x,t)].$$

Using the differentiation property of the Laplace transform, it yields

$$s^\alpha L[u] - \sum_{k=0}^{n-1} s^{\alpha-k-1} u^{(k)}(x,0) + L[Ru] + L[Nu] = L[g(x,t)].$$

On simplification, the above equation is reduced to

$$L[u] - \frac{1}{s^\alpha}\sum_{k=0}^{n-1} s^{\alpha-k-1} u^{(k)}(x,0) + \frac{1}{s^\alpha}(L[Ru] + L[Nu] - L[g(x,t)]) = 0.$$

We define the nonlinear operator as

$$N[\phi(x,t;q)] = L[\phi(x,t,q)] - \frac{1}{s^\alpha}\sum_{k=0}^{n-1} s^{\alpha-k-1}\phi^{(k)}(x,t,q)(0^+) + \frac{1}{s^\alpha}(L[R\phi(x,t,q)] + L[N\phi(x,t,q)] - L[g(x,t)]),$$

where $q \in [0, 1/n]$ and $\phi(x,t,q)$ are real functions of x, t and q. We construct a homotopy as follows:

$$(1-nq)L[\phi(x,t;q) - u_0(x,t)] = hqH(x,t)N[\phi(x,t;q)], \tag{3}$$

where L denotes the Laplace transform, $n \geq 1, q \in [0, 1/n]$ is the embedding parameter, $H(x,t)$ denotes a non-zero auxiliary function, $h \neq 0$ is an auxiliary parameter, $u_0(x,t)$ is an initial guess of $u(x,t)$ and $\phi(x,t;q)$ is an unknown function. It is obvious that when the embedding parameter $q = 0$ and $1/n$, it holds the result $\phi(x,t;0) = u_0(x,t)$ and $\phi(x,t;1/n) = u(x,t)$, respectively. Thus, as q increases from 0 to 1, the solution $\phi(x,t;q)$ varies from the initial guess $u_0(x,t)$ to the solution $u(x,t)$. Expanding the function $\phi(x,t;q)$ in the series form by applying Taylor's theorem about q, we have

$$\phi(x,t;q) = u_0(x,t) + \sum_{m=1}^{\infty} u_m(x,t)q^m, \tag{4}$$

where $u_m(x,t) = (1/m!)(\partial^m \phi(x,t;q)/\partial q^m)$.

If the auxiliary linear operator, the initial guess, the auxiliary parameter n, h and the auxiliary function H are properly chosen, series (4) converges at $q = 1/n$ and then, we have

$$u(x,t) = u_0(x,t) + \sum_{m=1}^{\infty} u_m(x,t)\left(\frac{1}{n}\right)^m,$$

which must be one of the solutions of the original nonlinear equations. According to the definition, the governing equation can be deduced from the zero-order deformation equation (3).

Define the vectors in the following manner: $\vec{u}_m = \{u_0(x,t), u_1(x,t), \ldots, u_m(x,t)\}$. Now, differentiating the zeroth-order deformation equation (3) m times with respect to q and then dividing them by $m!$ and finally setting $q = 0$, we get the following mth-order deformation equation:

$$L[u_m(x,t) - k_m u_m(x,t)] = hH(x,t)R_m(\vec{u}_{m-1}).$$

Finally, on applying the inverse Laplace transform, we have

$$u_m(x,t) = k_m u_m(x,t) + hL^{-1}[H(x,t)R_m(u_{m-1})],$$

where

$$k_m = \begin{cases} 0, & m \le 1, \\ n, & m > 1. \end{cases}$$

4. Convergence analysis of *q*-HATM

In this section, we presented the uniqueness and convergence analysis for the nonlinear time-FZK equation via q-HATM.

Theorem 1 (Uniqueness theorem) [47]. *The obtained solution with the aid of q-HATM for the FZK equation is unique wherever* $0 < \gamma < 1$, *where*

$$\gamma = (k_m + h) + h\big[\delta a(P^{p-1} + P^{p-2}Q^1 + \cdots + PQ^{p-2} + Q^{p-1}) + \delta^3 b(P^{q-1} + P^{q-2}Q^1 + \cdots + P^1Q^{q-2} + Q^{q-1}) + c\delta\delta_1^2(P^{r-1} + P^{r-2}Q^1 + \cdots + P^1Q^{r-2} + Q^{r-1})\big]\mu.$$

Proof. The solution for the FZK equation described in eq. (1) is represented as

$$u(x,t) = \sum_{m=0}^{\infty} u_m(x,t),$$

where

$$u_m(x,y,t) = (k_m + h)u_{m-1} - \left(1 - \frac{k_m}{n}\right)L^{-1}(g(x)) + hL^{-1}\big\{s^{-\beta}L[a\big(u^p\big)_x + b(u^q)_{xxx} + c(u^r)_{xyy}]\big\}.$$

If possible, let u and u^* be the two distinct solutions for the FZK equation such that $|u| \le P$ and $|u^*| \le Q$. Then, after using the above result, we obtain

$$|u - u^*| = |(k_m + h)\big(u - u^*\big) + hL^{-1}\{s^{-\beta}L[a((u^p)_x - (u^{*p})_x) + b((u^q)_{xxx} - (u^{*q})_{xxx}) + c((u^r)_{xyy} - (u^{*r})_{xyy})]\}|.$$

After applying the convolution theorem for Laplace transform (LT), we obtain

$$\begin{aligned}\big|u - u^*\big| &= (k_m + h)|(u - u^*)| + h\int_0^t [a|((u^p)_x - (u^{*p})_x)| + b|((u^q)_{xxx} - (u^{*q}l)_{xxx})| + c|((u^r)_{xyy} - (u^{*r})_{xyy})|]\frac{(t-\tau)^\beta}{\Gamma(\beta+1)}\,\mathrm{d}\tau \\ &\le (k_m + h)|(u - u^*)| + h\int_0^t [a|(u^p - u^{*p})_x| + b|(u^q - u^{*q})_{xxx}| + c|\big(u^r - u^{*r}\big)_{xyy}|]\frac{(t-\tau)^\beta}{\Gamma(\beta+1)}\,\mathrm{d}\tau.\end{aligned}$$

Let $\delta = \partial/\partial x, \delta_1 = \partial/\partial y, \delta^3 = \partial^3/\partial x^3, \delta\delta_1^2 = \partial^3/\partial x\partial^2 y$ and by using the integral mean value theorem, we obtain

$$\big|u - u^*\big| \le (k_m + h)|(u - u^*)|$$

$$
\begin{aligned}
&+h(\delta a|u^p-u^{*p}|+b\delta^3|u^q-u^{*q}|\\
&+c\delta\delta_1^2|u^r-u^{*r}|)\mu\\
&\le (k_m+h)|(u-u^*)|\\
&+h(\delta a|(u-u^*)(u^{p-1}\\
&+u^{p-2}u^{*1}+\cdots+u^1u^{*p-2}+u^{*p-1})|\\
&+b\delta^3|(u-u^*)(u^{q-1}+u^{q-2}u^{*1}+\cdots\\
&+u^1u^{*q-2}+u^{*q-1})|\\
&+c\delta\delta_1^2|(u-u^*)(u^{r-1}+u^{r-2}u^{*1}+\cdots\\
&+u^1u^{*r-2}+u^{*r-1})|)\mu\\
&\le (k_m+h)|(u-u^*)|\\
&+h[\delta a|(u-u^*)(P^{p-1}+P^{p-2}Q^1+\cdots\\
&+PQ^{p-2}+Q^{p-1})|\\
&+b\delta^3|(u-u^*)(P^{q-1}+P^{q-2}Q^1+\cdots\\
&+P^1Q^{q-2}+Q^{q-1})|\\
&+c\delta\delta_1^2|(u-u^*)(P^{r-1}+P^{r-2}Q^1+\cdots\\
&+P^1Q^{r-2}+Q^{r-1})|]\mu,
\end{aligned}
$$

$$\left|u-u^*\right|\le\gamma\left|u-u^*\right|,$$

$$(1-\gamma)\left|u-u^*\right|\le 0.$$

As $0<\gamma<1$, we get $|u-u^*|=0$, which gives $u=u^*$. This proves the uniqueness of the solution. □

Theorem 2 (Convergence theorem) [47]. *Suppose B is a Banach space and $T: B\to B$ is a nonlinear mapping such that*

$$\|T(v)-T(u)\|\le\gamma\|v-u\|,\quad \forall\, v,u\in B.$$

Then by Banach's fixed point theory [48,49] there is a fixed point for mapping T. Moreover, the sequence of the solution obtained by q-HATM converge to a fixed point T with an arbitrary choice of $v_0, u_0\in B$ and

$$\|u_m-u_n\|\le\frac{\gamma^n}{1-\gamma}\|u_1-u_0\|,\quad \forall\, v,u\in B.$$

Proof. Let $(C[f],\|\cdot\|)$ be a Banach space for all continuous functions on f with the norm symbolised as $\|g(t)\|=\max_{t\in f}|g(t)|$. First prove $\{u_n\}$ is a Cauchy sequence in the Banach space.

Now, consider

$$
\begin{aligned}
&\|u_m-u_n\|\\
&=\max_{t\in f}|u_m-u_n|\\
&=\max_{t\in f}|(k_m+h)(u_{m-1}-u_{n-1})\\
&+hL^{-1}\{s^{-\beta}L[a((u_{m-1}^p)_x-(u_{n-1}^p)_x)\\
&+b((u_{m-1}^q)_{xxx}-(u_{n-1}^q)_{xxx})\\
&+c((u_{m-1}^r)_{xyy}-(u_{n-1}^r)_{xyy})]\}|.
\end{aligned}
$$

After applying the convolution theorem for LT, we obtain

$$
\begin{aligned}
\|u_m-u_n\|\max_{t\in f}&\le (k_m+h)|(u_{m-1}-u_{n-1})|\\
&+h\int_0^t[a|((u_{m-1}^p)_x-(u_{n-1}^p)_x)|\\
&+b|((u_{m-1}^q)_{xxx}-(u_{n-1}^q)_{xxx})|\\
&+c|((u_{m-1}^r)_{xyy}-(u_{n-1}^r)_{xyy})|]\frac{(t-\tau)^\beta}{\Gamma(\beta+1)}\mathrm{d}\tau.
\end{aligned}
$$

Let $\delta=\partial/\partial x, \delta_1=\partial/\partial y, \delta^3=\partial^3/\partial x^3, \delta\delta_1^2=\partial^3/\partial x\partial^2 y$ and by using the integral mean value theorem [48,50], we obtain

$$
\begin{aligned}
\|u_m-u_n\|&\le\max_{t\in f}(k_m+h)|(u_{m-1}-u_{n-1})|\\
&+h\big[\delta a|(u_{m-1}-u_{n-1})(P^{p-1}\\
&+P^{p-2}Q^1+\cdots+PQ^{p-2}+Q^{p-1})|\\
&+b\delta^3|(u_{m-1}-u_{n-1})(P^{q-1}+P^{q-2}Q^1+\cdots\\
&+P^1Q^{q-2}+Q^{q-1})|\\
&+c\delta\delta_1^2|(u_{m-1}-u_{n-1})(P^{r-1}+P^{r-2}Q^1+\cdots\\
&+P^1Q^{r-2}+Q^{r-1})|]\mu,
\end{aligned}
$$

$$\|u_m-u_n\|\le\gamma\|u_{m-1}-u_{n-1}\|.$$

Putting $m=n+1$, it gives

$$
\begin{aligned}
\|u_{n+1}-u_n\|&\le\gamma\|u_n-u_{n-1}\|\\
&\le\gamma^2\|u_{n-1}-u_{n-2}\|\le\cdots\gamma^n\|u_1-u_0\|.
\end{aligned}
$$

On using triangular inequality, we get

$$
\begin{aligned}
\|u_m-u_n\|&\le\|u_{n+1}-u_n\|+\|u_{n+2}-u_{n+1}\|\\
&+\cdots+\|u_m-u_{m-1}\|\\
&\le\gamma^n\left[\frac{1-\gamma^{m-n-1}}{1-\gamma}\right]\|u_1-u_0\|.
\end{aligned}
$$

As $0<\gamma<1$, so $1-\gamma^{m-n-1}<1$. Then we get

$$\|u_m-u_n\|\le\gamma^n\left[\frac{\gamma^n}{1-\gamma}\right]\|u_1-u_0\|.$$

But $\|u_1-u_0\|<\infty$ and $m\to\infty$ then $\|u_m-u_n\|\to 0$, and consequently, the sequence $\{u_n\}$ is a Cauchy sequence in the Banach space $C[f]$ and sequence $\{u_n\}$ is convergent. This finalises our desired result. □

5. Numerical examples

In this section, we implement the proposed technique q-HATM on two different nonlinear time-FZK equations.

Example 1. In the present model, we study the nonlinear time-FZK (2, 2, 2) equation [40] as

$$D_t^{\beta} u + (u^2)_x + \frac{1}{8}(u^2)_{xxx} + \frac{1}{8}(u^2)_{xyy} = 0, \tag{5}$$

where $0 < \beta \leq 1$. The exact solution to eq. (5) when $\beta = 1$ and subject to the initial condition

$$u(x, y, 0) = \frac{4}{3}\rho \sinh^2(x + y),$$

where ρ is an arbitrary constant, was derived in [46] and is given as

$$u(x, y, t) = \frac{4}{3}\rho \sinh^2(x + y - \rho t).$$

Taking the Laplace transform on both sides of eq. (5), we obtain

$$s^{\beta}L[u] - s^{\beta-1}u(x, y, 0) + L\left[(u^2)_x + \frac{1}{8}(u^2)_{xxx} + \frac{1}{8}(u^2)_{xyy}\right] = 0$$

or

$$L[u] - \frac{1}{s}u(x, y, 0) + s^{-\beta}L\left[\left(u^2\right)_x + \frac{1}{8}\left(u^2\right)_{xxx} + \frac{1}{8}\left(u^2\right)_{xyy}\right] = 0.$$

We define the nonlinear operator as

$$N[\phi(x, t; q)] = L[\phi(x, t; q)] - \left(1 - \frac{k_m}{n}\right)\frac{4}{3s}\rho(\sinh[x + y])^2 + s^{-\beta}L\left[\left(\phi^2\right)_x + \frac{1}{8}\left(\phi^2\right)_{xxx} + \frac{1}{8}\left(\phi^2\right)_{xyy}\right].$$

The recursive scheme is

$$L\left[u_m(x, y, t) - k_m u_{m-1}(x, y, t)\right] = hR_m\left[u_{m-1}\right], \tag{6}$$

where

$$R_m[u_{m-1}] = L\left\{u_{m-1} - \left(1 - \frac{k_m}{n}\right)\frac{4}{3s}\rho(\sinh[x+y])^2 + s^{-\beta}L\left[\left(\sum_{k=0}^{m-1} u_{m-1-k}u_k\right)_x + \frac{1}{8}\left(\sum_{k=0}^{m-1} u_{m-1-k}u_k\right)_{xxx} + \frac{1}{8}\left(\sum_{k=0}^{m-1} u_{m-1-k}u_k\right)_{xyy}\right]\right\}. \tag{7}$$

Applying the inverse Laplace transform to eq. (6) and using (7), we obtain

$$u_m(x, y, t) = (k_m + h)u_{m-1} - \frac{4h}{3}\rho \sinh^2(x + y)\left(1 - \frac{k_m}{n}\right) + hL^{-1}\left\{s^{-\beta}L\left[\left(\sum_{k=0}^{m-1} u_{m-1-k}u_k\right)_x + \frac{1}{8}\left(\sum_{k=0}^{m-1} u_{m-1-k}u_k\right)_{xxx} + \frac{1}{8}\left(\sum_{k=0}^{m-1} u_{m-1-k}u_k\right)_{xyy}\right]\right\}.$$

By putting $m = 1, 2, 3, \ldots,$ we obtain

$$u_1(x, y, t) = h\left[\frac{224}{9}\rho^2 \sinh^3(x + y)\cosh(x + y) + \frac{32}{3}\rho^2\sinh(x + y)\cosh^3(x + y)\right]\frac{t^{\beta}}{\Gamma(\beta + 1)},$$

$$u_2(x, y, t) = (h + n)u_1 + hL^{-1}\left\{s^{-\beta}L\left[\left(\sum_{k=0}^{1} u_{1-k}u_k\right)_x + \frac{1}{8}\left(\sum_{k=0}^{1} u_{1-k}u_k\right)_{xxx} + \frac{1}{8}\left(\sum_{k=0}^{1} u_{1-k}u_k\right)_{xyy}\right]\right\}$$

$$= \frac{64}{27}h^2\rho^3[2400\cosh^6(x+y) - 4160\cosh^4(x+y) + 1936\cosh^2(x + y) - 158]\frac{t^{2\beta}}{\Gamma(2\beta + 1)} + h(h + n)\left[\frac{224}{9}\rho^2 \sinh^3(x + y)\cosh(x + y) + \frac{32}{3}\rho^2\sinh(x + y)\cosh^3(x + y)\right]\frac{t^{\beta}}{\Gamma(\beta + 1)},$$

$$
\begin{aligned}
u_3(x,y,t) &= (h+n)u_2 \\
&\quad + hL^{-1}\left\{ s^{-\beta} L\left[\left(\sum_{k=0}^{2} u_{2-k}u_k\right)_x \right.\right. \\
&\quad \left.\left. + \frac{1}{8}\left(\sum_{k=0}^{2} u_{2-k}u_k\right)_{xxx} + \frac{1}{8}\left(\sum_{k=0}^{2} u_{2-k}u_k\right)_{xyy} \right]\right\} \\
&= h^2(1+h)\rho^3 \frac{4}{3}\left\{ \frac{121192}{9}\sinh^2(x+y)\cosh^4(x+y) \right. \\
&\quad + \frac{23392}{9}\sinh^4(x+y)\cosh^2(x+y) \\
&\quad + \frac{2528}{9}\sinh^6(x+y) \\
&\quad \left. + \frac{288}{9}\cosh^6(x+y) \right\} \frac{t^{2\beta}}{\Gamma(2\beta+1)} \\
&\quad + h^3\rho^4 \frac{256}{9}\{403200 \\
&\quad \times \sinh^3(x+y)\cosh^5(x+y) \\
&\quad + 144000\sinh^5(x+y)\cosh^3(x+y) \\
&\quad + 105600\sinh(x+y)\cosh^7(x+y) \\
&\quad - 49920\sinh^5(x+y)\cosh(x+y) \\
&\quad - 133120\sinh(x+y)\cosh^5(x+y) \\
&\quad - 316160\sinh^3(x+y)\cosh^3(x+y) \\
&\quad + 38716\sinh^3(x+y)\cosh(x+y) \\
&\quad + 38716\sinh(x+y)\cosh^3(x+y) \\
&\quad - 1264\sinh(x+y)\cosh(x+y)\} \frac{t^{3\beta}}{\Gamma(3\beta+1)} \\
&\quad + h^3\rho^4 \left\{ \frac{50176}{81}[30\sinh^3(x+y) \right. \\
&\quad \times \cosh^5(x+y) + 84\sinh^5(x+y)\cosh^3(x+y) \\
&\quad + 22\sinh^7(x+y)\cosh(x+y)] \\
&\quad + \frac{1024}{9}[22\sinh(x+y)\cosh^7(x+y) \\
&\quad + 84\sinh^3(x+y)\cosh^5(x+y) \\
&\quad + 20\sinh^5(x+y)\cosh^3(x+y)] \\
&\quad + \frac{14336}{27}[6\sinh(x+y)\cosh^7(x+y) \\
&\quad + 6\sinh^7(x+y)\cosh(x+y) \\
&\quad + 52\sinh^5(x+y)\cosh^3(x+y) \\
&\quad \left. + 52\sinh^3(x+y)\cosh^5(x+y)] \right\}
\end{aligned}
$$

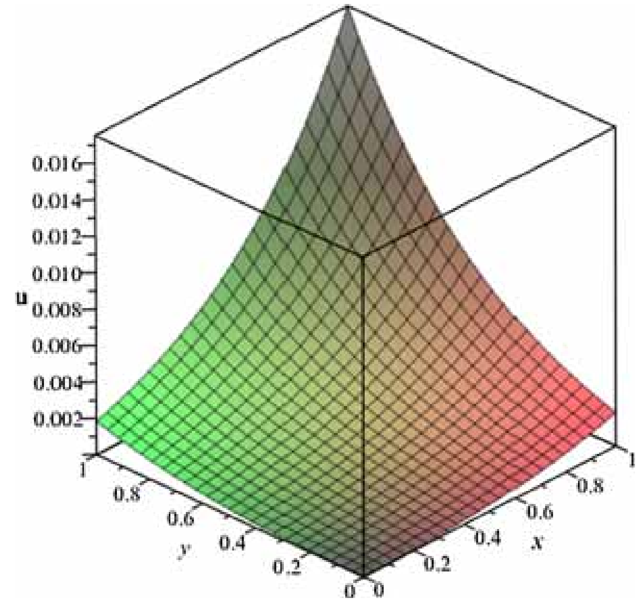

Figure 1. The surface shows exact solution when $t = 0.5$, $n = 1$, $h = -1$ and $\rho = 0.001$, for Example 1.

$$
\begin{aligned}
&\times \frac{\Gamma(2\beta+1)t^{3\beta}}{(\Gamma(\beta+1))^2\Gamma(3\beta+1)} + \frac{64}{27}h^2(h+n)\rho^3 \\
&\times [2400\cosh^6(x+y) - 4160\cosh^4(x+y) \\
&+ 1936\cosh^2(x+y) - 158]\frac{t^{2\beta}}{\Gamma(2\beta+1)} \\
&+ h(h+n)^2\left[\frac{224}{9}\rho^2\sinh^3(x+y)\cosh(x+y) \right. \\
&\left. + \frac{32}{3}\rho^2\sinh(x+y)\cosh^3(x+y)\right]\frac{t^{\beta}}{\Gamma(\beta+1)}.
\end{aligned}
$$

Proceeding in the same manner, the rest of the components of the q-HATM solution can be obtained. Thus the solution $u(x, y, t)$ of eq. (5) is given as $u(x, y, t) = \sum_{k=0}^{\infty} u_k(1/n)^k$.

In a particular case, when we put $n = 1$ and $h = -1$, we obtain $u(x, y, t) = (4/3)\rho\sinh^2(x + y - \rho t)$, which is the exact solution to eq. (5) for $\beta = 1$.

Figure 1 shows the exact solution and figure 2 depicts the third-order q-HATM solution. It can be seen from figures 1 and 2 that the solution obtained by q-HATM is nearly identical with the exact solution. Figure 3 depicts the approximate solution when $\beta = 0.7, h = -1, t = 0.5$ and $\rho = 0.001$. Figure 4 represents the approximate solution when $c = 0.9, h = -1, t = 0.5$ and $\rho = 0.001$. Figure 5 shows the absolute error when $\beta = 1, h = -1, t = 0.5, \rho = 0.001$ and $n = 1$. Figure 6 represents the q-HATM solution for different values of β. Figure 7 presents the asymptotic n-curve for

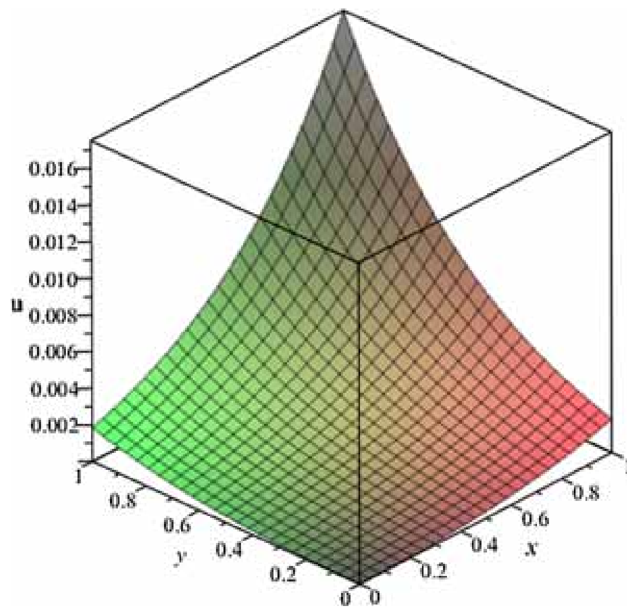

Figure 2. The surface shows q-HATM solution when $t = 0.5$, $n = 1$, $h = -1$, $\rho = 0.001$ and $\beta = 1$, for Example 1.

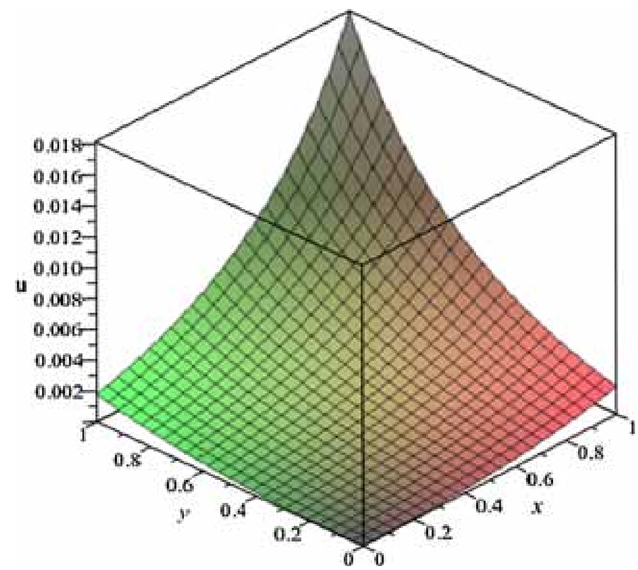

Figure 4. The surface shows q-HATM solution when $t = 0.5$, $n = 1$, $h = -1$, $\rho = 0.001$ and $\beta = 0.9$, for Example 1.

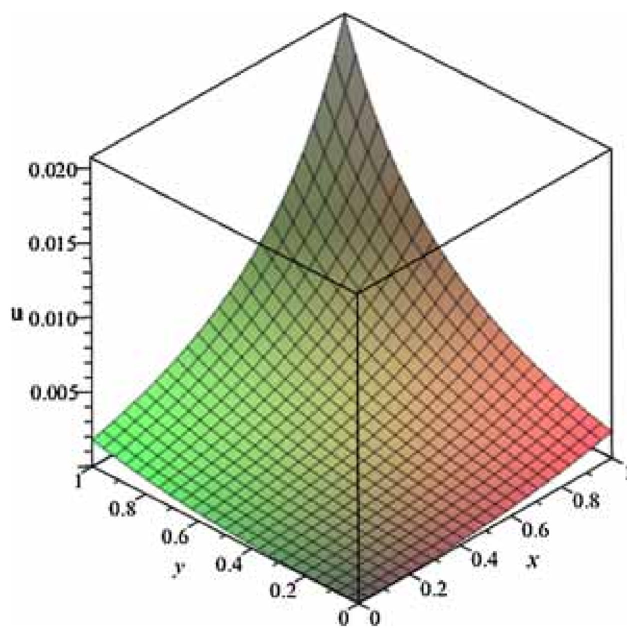

Figure 3. The surface shows q-HATM solution when $t = 0.5$, $n = 1$, $h = -1$, $\rho = 0.001$ and $\beta = 0.7$, for Example 1.

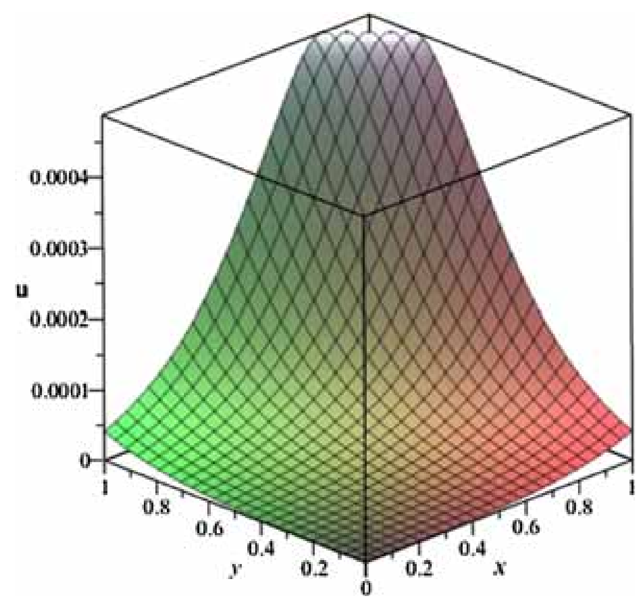

Figure 5. The surface shows $|u_{\mathrm{ex}} - u_{q\text{-HATM}}|$ when $t = 0.5$, $n = 1$, $h = -1$, $\rho = 0.001$ and $\beta = 1$, for Example 1.

different values of β and figures 8 and 9 represent the h-curve for different values of β and n for Example 1. The horizontal straight line in figures 8 and 9 shows the range of convergence. It is seen from figures 8 and 9 that as the value of β increases, the range of convergence increases and the value of n increases, and then, the range of convergence also increases. Here third-order approximation $u_3(x, y, t)$ is used to depict figures 6–9 and the second-order approximation $u_2(x, y, t)$ is used to evaluate tables 1– 3. Approximate solution and efficiency of q-HATM can be enhanced by computing higher-order approximations. Table 1 represents the comparison of the absolute errors among different methods. Tables 2 and 3 show the absolute errors between the exact solution and the approximate solution for different values of h and n.

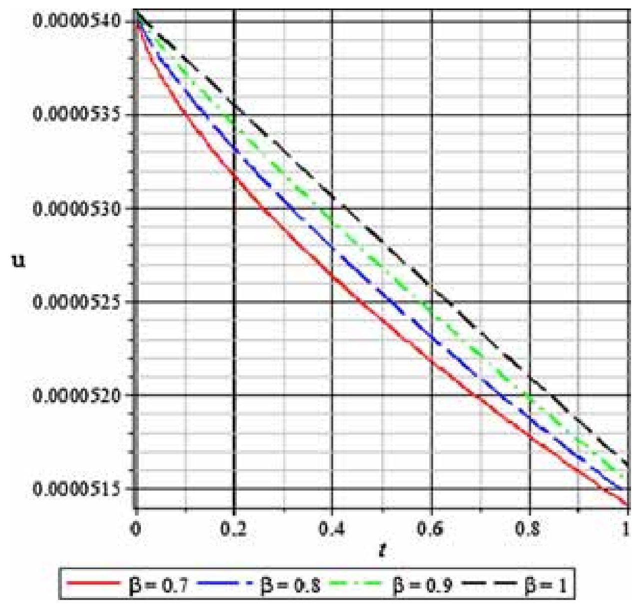

Figure 6. Plot of q-HATM solution for different values of β at $x = 0.1$, $y = 0.1$, $h = -1$ and $n = 1$, for Example 1.

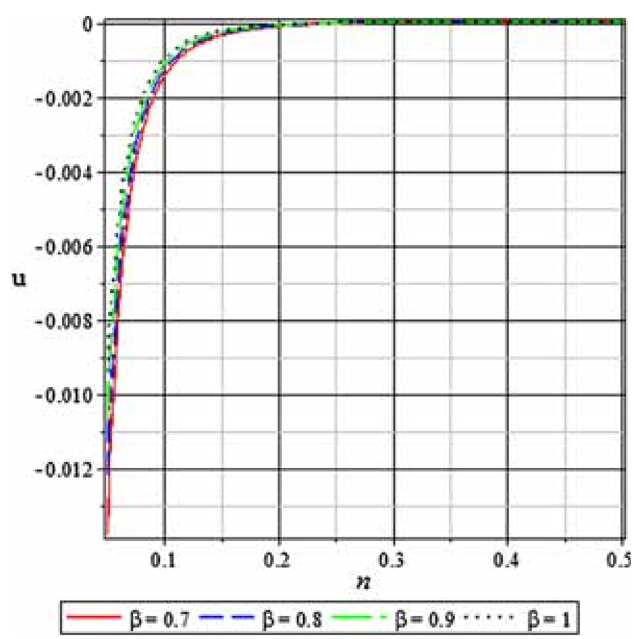

Figure 7. Plot of n-curve of q-HATM solution for different values of β at $t = 0.5$, $x = 0.1$, $y = 0.1$ and $h = -1$, for Example 1.

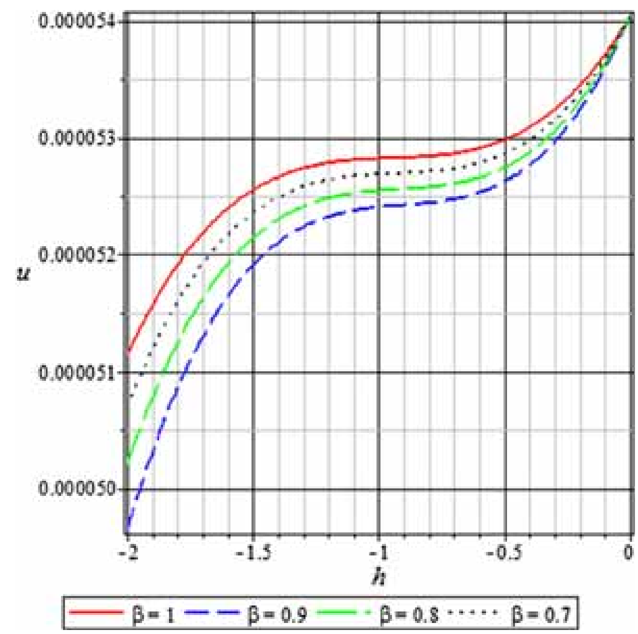

Figure 8. h-curve of q-HATM solution for different values of β at $t = 0.5$, $x = 0.1$, $y = 0.1$ and $n = 1$, for Example 1.

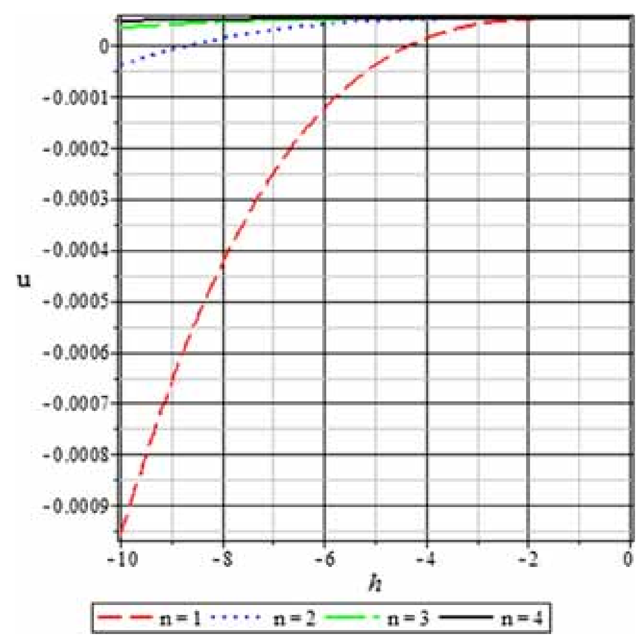

Figure 9. h-curve of q-HATM solution for different values of n at $t = 0.5$, $x = 0.1$, $y = 0.1$ and $\beta = 1$, for Example 1.

Example 2. In the present model, we study the nonlinear time-FZK (3, 3, 3) equation [40] as

$$D_t^{\beta} u + (u^3)_x + 2(u^3)_{xxx} + 2(u^3)_{xyy} = 0, \;\; 0 < \beta \leq 1. \tag{8}$$

The exact solution to eq. (8) when $\beta = 1$, subject to the initial condition

$$u(x, y, 0) = \frac{3}{2}\rho \sinh\left(\frac{1}{6}(x + y)\right),$$

where ρ is an arbitrary constant, was derived in [46] and is given as

$$u(x, y, t) = \frac{3}{2}\rho \sinh\left(\frac{x + y - \rho t}{6}\right).$$

Table 1. Comparison between absolute error when $t = 1, \beta = 1, h = -1, n = 1$ and $\rho = 0.001$, for Example 1.

	y	x					
		0	0.02	0.04	0.06	0.08	0.10
q-HATM	0.00	2.00×10^{-8}	1.40×10^{-7}	3.01×10^{-7}	4.66×10^{-7}	6.35×10^{-7}	8.12×10^{-7}
LDM		2.00×10^{-8}	1.40×10^{-7}	3.01×10^{-7}	4.66×10^{-7}	6.35×10^{-7}	8.12×10^{-7}
VIM [28]		2.00×10^{-8}	3.95×10^{-6}	7.90×10^{-6}	1.19×10^{-5}	1.59×10^{-5}	2.00×10^{-5}
HPTM [30]		2.00×10^{-8}	1.40×10^{-7}	3.01×10^{-7}	4.65×10^{-7}	6.35×10^{-7}	8.12×10^{-7}
q-HATM	0.02	1.40×10^{-7}	3.01×10^{-7}	4.66×10^{-7}	6.35×10^{-7}	8.12×10^{-7}	9.98×10^{-7}
LDM		1.40×10^{-7}	3.01×10^{-7}	4.66×10^{-7}	6.35×10^{-7}	8.12×10^{-7}	9.98×10^{-7}
VIM [28]		3.95×10^{-6}	7.90×10^{-6}	1.19×10^{-5}	1.59×10^{-5}	2.00×10^{-5}	2.41×10^{-5}
HPTM [30]		1.40×10^{-7}	3.01×10^{-7}	4.65×10^{-7}	6.35×10^{-7}	8.11×10^{-7}	9.98×10^{-7}
q-HATM	0.04	3.01×10^{-7}	4.66×10^{-7}	6.35×10^{-7}	8.12×10^{-7}	9.98×10^{-7}	1.20×10^{-6}
LDM		3.01×10^{-7}	4.66×10^{-7}	6.35×10^{-7}	8.12×10^{-7}	9.98×10^{-7}	1.20×10^{-6}
VIM [28]		7.90×10^{-6}	1.19×10^{-5}	1.59×10^{-5}	2.00×10^{-5}	2.41×10^{-5}	2.84×10^{-5}
HPTM [30]		3.01×10^{-7}	4.66×10^{-7}	6.35×10^{-7}	8.12×10^{-7}	9.98×10^{-7}	1.20×10^{-6}
q-HATM	0.06	4.66×10^{-7}	6.35×10^{-7}	8.12×10^{-7}	9.98×10^{-7}	1.20×10^{-6}	1.41×10^{-6}
LDM		4.66×10^{-7}	6.35×10^{-7}	8.12×10^{-7}	9.98×10^{-7}	1.20×10^{-6}	1.41×10^{-6}
VIM [30]		1.19×10^{-5}	1.59×10^{-5}	2.00×10^{-5}	2.41×10^{-5}	2.84×10^{-5}	3.27×10^{-5}
HPTM [32]		4.66×10^{-7}	6.35×10^{-7}	8.12×10^{-7}	9.98×10^{-7}	1.20×10^{-6}	1.41×10^{-6}
q-HATM	0.08	6.35×10^{-7}	8.12×10^{-7}	9.98×10^{-7}	1.20×10^{-6}	1.41×10^{-6}	1.63×10^{-6}
LDM		6.35×10^{-7}	8.12×10^{-7}	9.98×10^{-7}	1.20×10^{-6}	1.41×10^{-6}	1.63×10^{-6}
VIM [28]		1.59×10^{-5}	2.00×10^{-5}	2.41×10^{-5}	2.84×10^{-5}	3.27×10^{-5}	3.72×10^{-5}
HPTM [30]		6.35×10^{-7}	8.12×10^{-7}	9.98×10^{-7}	1.20×10^{-6}	1.41×10^{-6}	1.63×10^{-6}
q-HATM	0.10	8.12×10^{-7}	9.98×10^{-7}	1.20×10^{-6}	1.41×10^{-6}	1.63×10^{-6}	1.88×10^{-6}
LDM		8.12×10^{-7}	9.98×10^{-7}	1.20×10^{-6}	1.41×10^{-6}	1.63×10^{-6}	1.88×10^{-6}
VIM [28]		2.00×10^{-5}	2.41×10^{-5}	2.84×10^{-5}	3.27×10^{-5}	3.72×10^{-5}	4.18×10^{-5}
HPTM [30]		8.12×10^{-7}	9.98×10^{-7}	1.20×10^{-6}	1.41×10^{-6}	1.63×10^{-6}	1.88×10^{-6}

Table 2. Absolute error $|u - u_2|$ when $t = 1, \beta = 1, h = -1.9, n = 2$ and $\rho = 0.001$, for Example 1.

y	x					
	0.00	0.02	0.04	0.06	0.08	0.1
0.00	1.79×10^{-8}	3.89×10^{-7}	1.60×10^{-6}	3.61×10^{-6}	6.42×10^{-6}	1.00×10^{-5}
0.02	3.89×10^{-7}	1.60×10^{-6}	3.61×10^{-6}	6.42×10^{-6}	1.00×10^{-5}	1.45×10^{-5}
0.04	1.60×10^{-6}	3.61×10^{-6}	6.42×10^{-6}	1.00×10^{-5}	1.45×10^{-5}	1.98×10^{-5}
0.06	3.61×10^{-6}	6.42×10^{-6}	1.00×10^{-5}	1.45×10^{-5}	1.98×10^{-5}	2.59×10^{-5}
0.08	6.42×10^{-6}	1.00×10^{-5}	1.45×10^{-5}	1.98×10^{-5}	2.59×10^{-5}	3.28×10^{-5}
0.10	1.00×10^{-5}	1.45×10^{-5}	1.98×10^{-5}	2.59×10^{-5}	3.28×10^{-5}	4.06×10^{-5}

Table 3. Absolute error $|u - u_2|$ when $t = 1, \beta = 1, h = -2.9, n = 3$ and $\rho = 0.001$, for Example 1.

y	x					
	0	0.02	0.04	0.06	0.08	0.1
0.00	1.86×10^{-8}	4.32×10^{-7}	1.83×10^{-6}	4.18×10^{-6}	7.48×10^{-6}	1.17×10^{-5}
0.02	4.32×10^{-7}	1.83×10^{-6}	4.18×10^{-6}	7.48×10^{-6}	1.17×10^{-5}	1.70×10^{-5}
0.04	1.83×10^{-6}	4.18×10^{-6}	7.48×10^{-6}	1.17×10^{-5}	1.70×10^{-5}	2.32×10^{-5}
0.06	4.18×10^{-6}	7.48×10^{-6}	1.17×10^{-5}	1.70×10^{-5}	2.32×10^{-5}	3.04×10^{-5}
0.08	7.48×10^{-6}	1.17×10^{-5}	1.70×10^{-5}	2.32×10^{-5}	3.04×10^{-5}	3.86×10^{-5}
0.10	1.17×10^{-5}	1.70×10^{-5}	2.32×10^{-5}	3.04×10^{-5}	3.86×10^{-5}	4.78×10^{-5}

Taking the Laplace transform on both sides of eq. (8), we obtain

$$s^{\beta}L[u]-s^{\beta-1}\frac{3}{2}\rho\sinh\left(\frac{x+y}{6}\right)+L[(u^3)_x+2(u^3)_{xxx}+2(u^3)_{xyy}]=0$$

or

$$L[u]-\frac{1}{s}\frac{3}{2}\rho\sinh\left(\frac{x+y}{6}\right)+s^{\beta-1}L[(u^3)_x+2(u^3)_{xxx}+2(u^3)_{xyy}]=0.$$

We define the nonlinear operator as

$$N[\phi(x,t;q)]=L[\phi(x,t;q)]-\left(1-\frac{k_m}{n}\right)\frac{3}{2s}\rho\sinh\left(\frac{x+y}{6}\right)+s^{\beta-1}L\left[(\phi^3)_x+2(\phi^3)_{xxx}+2(\phi^3)_{xyy}\right].$$

The recursive formula is

$$L\left[u_m(x,y,t)-k_m u_{m-1}(x,y,t)\right]=hR_m\left[u_{m-1}\right], \tag{9}$$

where

$$R_m[u_{m-1}] = L\left\{u_{m-1}-\left(1-\frac{k_m}{n}\right)\frac{1}{s}\frac{3}{2}\rho\sinh\left(\frac{x+y}{6}\right) + s^{-\beta}L\left[\left(\sum_{i=0}^{m-1}u_i\sum_{j=0}^{m-1-i}u_ju_{m-1-i-j}\right)_x + 2\left(\sum_{i=0}^{m-1}u_i\sum_{j=0}^{m-1-i}u_ju_{m-1-i-j}\right)_{xxx} + 2\left(\sum_{i=0}^{m-1}u_i\sum_{j=0}^{m-1-i}u_ju_{m-1-i-j}\right)_{xyy}\right]\right\}. \tag{10}$$

Applying the inverse Laplace transform of eq. (9), we obtain

$$u_m(x,y,t)=(k_m+h)u_{m-1} - h\frac{3}{2}\rho\sinh\left(\frac{x+y}{6}\right)\left(1-\frac{k_m}{n}\right) + hL^{-1}\left\{s^{-\beta}L\left[\left(\sum_{i=0}^{m-1}u_i\sum_{j=0}^{m-1-i}u_ju_{m-1-i-j}\right)_x + 2\left(\sum_{i=0}^{m-1}u_i\sum_{j=0}^{m-1-i}u_ju_{m-1-i-j}\right)_{xxx} + 2\left(\sum_{i=0}^{m-1}u_i\sum_{j=0}^{m-1-i}u_ju_{m-1-i-j}\right)_{xyy}\right]\right\}.$$

By putting $m=1,2,3,\ldots,$ we obtain

$$u_1(x,y,t) = 3h\rho^3\left[\sinh^3\frac{1}{6}(x+y)\right]\cosh\left[\frac{1}{6}(x+y)\right] + \frac{1}{8}\cosh^3\left[\frac{1}{6}(x+y)\right]\frac{t^{\beta}}{\Gamma(\beta+1)},$$

$$u_2(x,y,t) = (h+n)u_1 + hL^{-1}\left\{s^{-\beta}L\left[\left(\sum_{i=0}^{1}u_i\sum_{j=0}^{1-i}u_ju_{m-1-i-j}\right)_x + 2\left(\sum_{i=0}^{1}u_i\sum_{j=0}^{1-i}u_ju_{m-1-i-j}\right)_{xxx} + 2\left(\sum_{i=0}^{1}u_i\sum_{j=0}^{1-i}u_ju_{1-i-j}\right)_{xyy}\right]\right\}$$

$$= \frac{3}{64}\rho^5h^2\sinh\left[\frac{1}{6}(x+y)\right]\left\{1530\cosh^4\left[\frac{1}{6}(x+y)\right] - 1458\cosh^2\left[\frac{1}{6}(x+y)\right] + 182\right\}\frac{t^{2\beta}}{\Gamma(2\beta+1)} + 3h(h+n)\rho^3\left\{\sinh^3\left[\frac{1}{6}(x+y)\right]\times\cosh\left[\frac{1}{6}(x+y)\right] + \frac{1}{8}\cosh^3\left[\frac{1}{6}(x+y)\right]\right\}\frac{t^{\beta}}{\Gamma(\beta+1)},$$

$$u_3(x,y,t) = (h+n)u_2 + hL^{-1}\left\{s^{-\beta}L\left[\left(\sum_{i=0}^{2}u_i\sum_{j=0}^{2-i}u_ju_{m-1-i-j}\right)_x\right.\right.$$

$$
\begin{aligned}
&+2\left(\sum_{i=0}^{2}u_i\sum_{j=0}^{2-i}u_ju_{m-1-i-j}\right)_{xxx}\\
&+2\left(\sum_{i=0}^{2}u_i\sum_{j=0}^{2-i}u_ju_{1-i-j}\right)_{xyy}\Bigg]\Bigg\}\\
&=\frac{27}{1536}\rho^7h^3\frac{t^{3\beta}}{\Gamma(3\beta+1)}\left\{3060\cosh^7\left[\frac{1}{6}(x+y)\right]\right.\\
&+79560\cosh^5\left[\frac{1}{6}(x+y)\right]\sinh^2\left[\frac{1}{6}(x+y)\right]\\
&+112200\cosh^3\left[\frac{1}{6}(x+y)\right]\sinh^4\left[\frac{1}{6}(x+y)\right]\\
&+12240\cosh\left[\frac{1}{6}(x+y)\right]\sinh^6\left[\frac{1}{6}(x+y)\right]\\
&-30132\cosh\left[\frac{1}{6}(x+y)\right]\sinh^4\left[\frac{1}{6}(x+y)\right]\\
&-49572\cosh^3\left[\frac{1}{6}(x+y)\right]\sinh^2\left[\frac{1}{6}(x+y)\right]\\
&-2916\cosh^5\left[\frac{1}{6}(x+y)\right]\\
&+2915\cosh\left[\frac{1}{6}(x+y)\right]\sinh^2\left[\frac{1}{6}(x+y)\right]\\
&\left.+364\cosh^3\left[\frac{1}{6}(x+y)\right]\right\}\\
&+\frac{27}{12}\rho^5h^3\frac{\Gamma(2\beta+1)t^{3\beta}}{\Gamma(3\beta+1)(\Gamma(\beta+1))^2}\\
&\times 70\left\{\cosh^5\left[\frac{1}{6}(x+y)\right]\sinh^4\left[\frac{1}{6}(x+y)\right]\right.\\
&+\frac{490}{3}\cosh^3\left[\frac{1}{6}(x+y)\right]\sinh^6\left[\frac{1}{6}(x+y)\right]\\
&+\frac{110}{3}\cosh\left[\frac{1}{6}(x+y)\right]\sinh^8\left[\frac{1}{6}(x+y)\right]\\
&+\frac{84}{64}\cosh^5\left[\frac{1}{6}(x+y)\sinh^2\left[\frac{1}{6}(x+y)\right]\right.\\
&+\frac{28}{192}\cosh^7\left[\frac{1}{6}(x+y)\right]\\
&+\frac{40}{64}\cosh^3\left[\frac{1}{6}(x+y)\right]\sinh^4\left[\frac{1}{6}(x+y)\right]\\
&+2\cosh^6\left[\frac{1}{6}(x+y)\right]\sinh\left[\frac{1}{6}(x+y)\right]\\
&+\frac{67}{3}\cosh^5\left[\frac{1}{6}(x+y)\right]\sinh^3\left[\frac{1}{6}(x+y)\right]\\
&+\frac{67}{3}\cosh^3\left[\frac{1}{6}(x+y)\right]\sinh^5\left[\frac{1}{6}(x+y)\right]\\
&\left.+2\cosh\left[\frac{1}{6}(x+y)\right]\sinh^7\left[\frac{1}{6}(x+y)\right]\right\}\\
&+\frac{27}{24}\rho^5h^2(h+n)\frac{t^{2\beta}}{\Gamma(2\beta+1)}\\
&\times\left\{20\sinh^2\left[\frac{1}{6}(x+y)\right]\cosh^4\left[\frac{1}{6}(x+y)\right]\right.\\
&+\frac{185}{3}\cosh^2\left[\frac{1}{6}(x+y)\right]\sinh^4\left[\frac{1}{6}(x+y)\right]\\
&+\frac{25}{3}\sinh^6\left[\frac{1}{6}(x+y)\right]\\
&+\frac{62}{24}\cosh^4\left[\frac{1}{6}(x+y)\right]\sinh\left[\frac{1}{6}(x+y)\right]\\
&+\frac{34}{8}\cosh^2\left[\frac{1}{6}(x+y)\right]\sinh^3\left[\frac{1}{6}(x+y)\right]\\
&\left.+\frac{2}{8}\sinh^5\left[\frac{1}{6}(x+y)\right]\right\}+\frac{3}{64}\rho^5(h+n)h^2\\
&\times\sinh\left[\frac{1}{6}(x+y)\right]\left\{1530\cosh^4\left[\frac{1}{6}(x+y)\right]\right.\\
&\left.-1458\cosh^2\left[\frac{1}{6}(x+y)\right]+182\right\}\frac{t^{2\beta}}{\Gamma(2\beta+1)}\\
&+3h(h+n)^2\rho^3\left\{\sinh^3\left[\frac{1}{6}(x+y)\right]\right.\\
&\times\cosh\left[\frac{1}{6}(x+y)\right]\\
&\left.+\frac{1}{8}\cosh^3\left[\frac{1}{6}(x+y)\right]\right\}\frac{t^{\beta}}{\Gamma(\beta+1)}.
\end{aligned}
$$

Proceeding in the same manner, the rest of the components of the q-HATM solution can be obtained. Thus, the solution $u(x, y, t)$ of eq. (8) is given as

$$u(x, y, t) = \sum_{k=0}^{\infty} u_k \left(\frac{1}{n}\right)^k.$$

In a particular case, when we use $n = 1$ and $h = -1$, we obtain

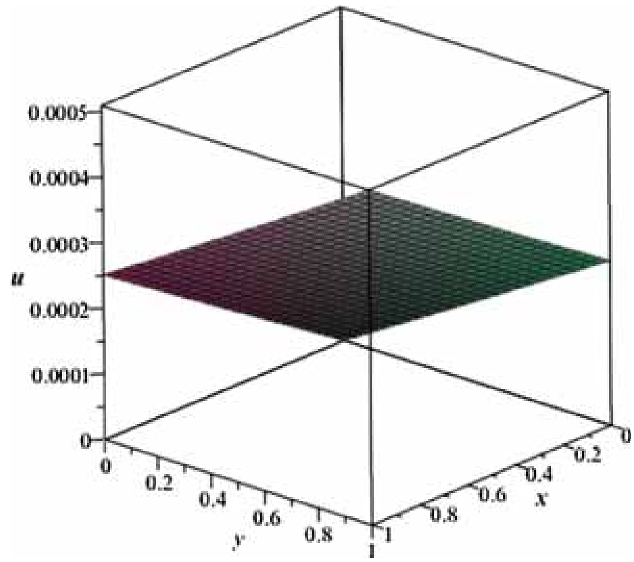

Figure 10. The surface shows exact solution when $t = 0.5$, $n = 1$, $h = -1$ and $\rho = 0.001$, for Example 2.

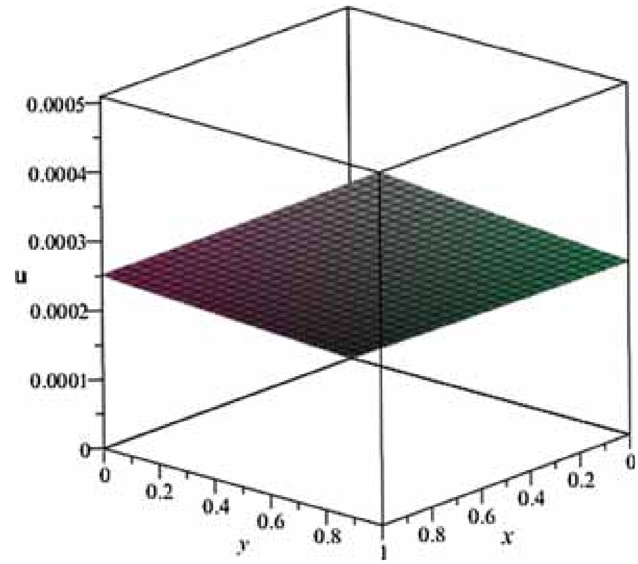

Figure 12. The surface shows q-HATM solution when $t = 0.5$, $n = 1$, $h = -1$, $\rho = 0.001$ and $\beta = 0.7$, for Example 2.

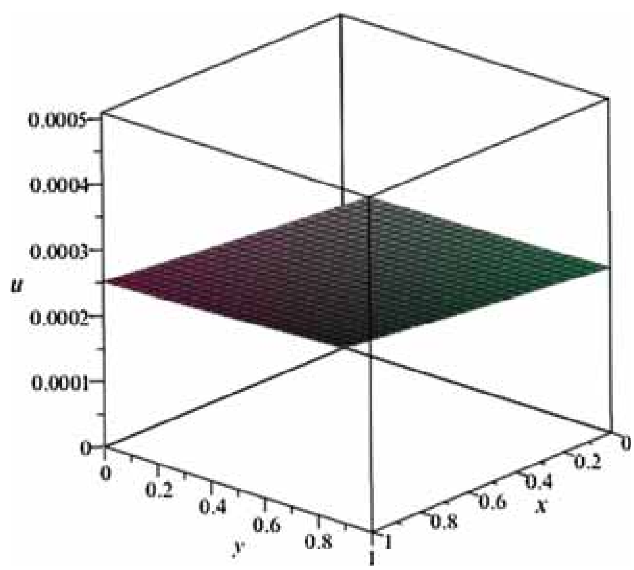

Figure 11. The surface shows q-HATM solution when $t = 0.5$, $n = 1$, $h = -1$, $\rho = 0.001$ and $\beta = 1$, for Example 2.

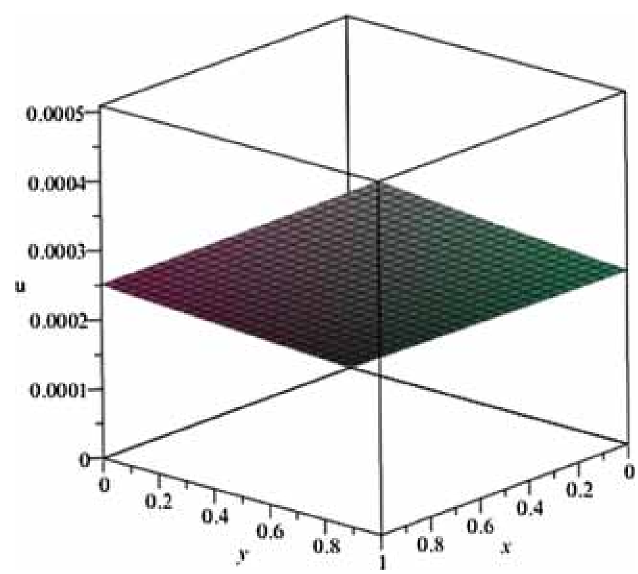

Figure 13. The surface shows q-HATM solution when $t = 0.5$, $n = 1$, $h = -1$, $\rho = 0.001$ and $\beta = 0.9$, for Example 2.

$$u(x, y, t) = \frac{3}{2}\rho \sinh\left(\frac{x + y - \rho t}{6}\right),$$

which is the exact solution to eq. (8) for $\beta = 1$.

Figure 10 shows the exact solution and figure 11 depicts the third-order approximate q-HATM solution. It can be seen from figures 10 and 11 that the solution obtained by q-HATM is nearly identical with the exact solution. Figure 12 depicts the approximate solution when $\beta = 0.7, h = -1, t = 0.5$ and $\rho = 0.001$. Figure 13 represents the approximate solution when $c = 0.9, h = -1, t = 0.5$ and $\rho = 0.001$. Figure 14 shows the absolute error when $\beta = 1$, $h = -1, t = 0.5, \rho = 0.001$ and $n = 1$. Figure 15 represents the q-HATM solution for different values of β. Figure 16 presents the asymptotic n-curve for different values of β and figures 17 and 18 represent the h-curve for different values of β and n for Example 2. The horizontal straight line in figures 17 and 18 shows the range of convergence. It is seen from figures 17 and 18 that

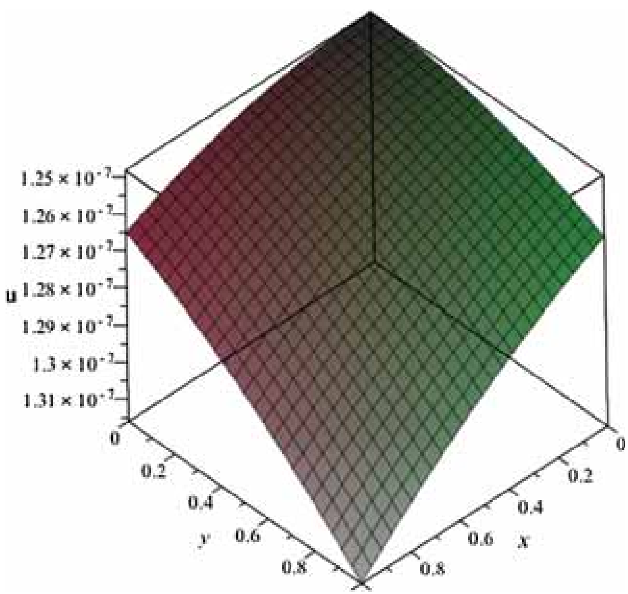

Figure 14. The surface shows $|u_{\text{ex}} - u_{q\text{-HATM}}|$ when $t = 0.5, n = 1, h = -1, \rho = 0.001$ and $\beta = 1$, for Example 2.

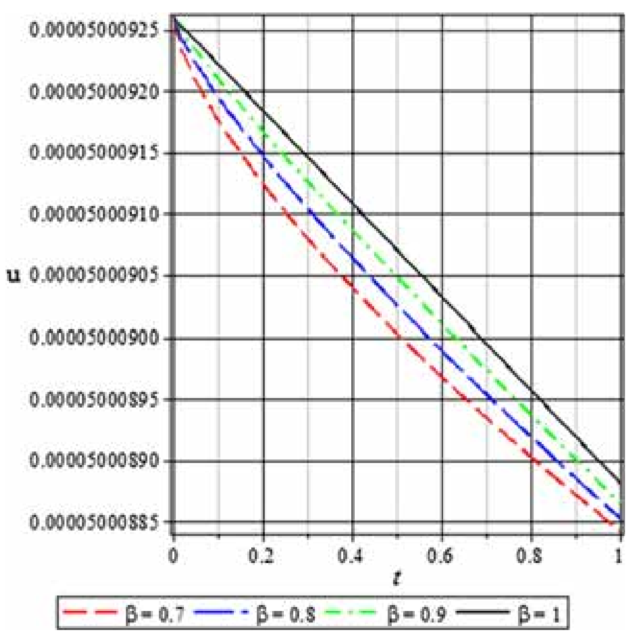

Figure 15. Plot of q-HATM solution for different values of β at $x = 0.1$, $y = 0.1$, $h = -1$ and $n = 1$, for Example 2.

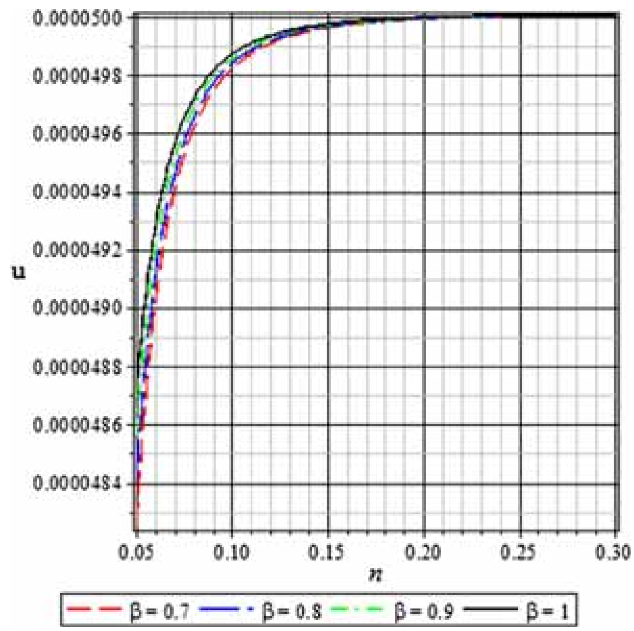

Figure 16. Plot of n-curve of q-HATM solution for different values of β at $t = 0.5, x = 0.1, y = 0.1$ and $h = -1$, for Example 2.

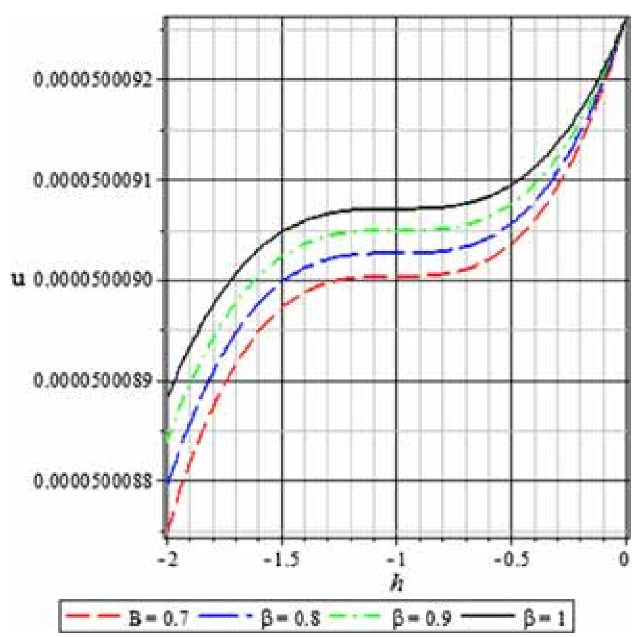

Figure 17. h-curve of q-HATM solution for different values of β at $t = 0.5$, $x = 0.1$, $y = 0.1$ and $n = 1$, for Example 2.

as the value of β increases, the range of convergence increases and the value of n increases, then the range of convergence also increases. Here the third-order approximation $u_3(x, y, t)$ is used to depict figures 15–18 and the second-order approximation $u_2(x, y, t)$ is used to evaluate tables 4–8. The approximate solution and efficiency of q-HATM can be enhanced by computing higher-order approximations. Table 4 represents the comparison of the absolute error of different methods. Tables 5–8 show the absolute error between the exact solution and the approximate solution for different values of h and n.

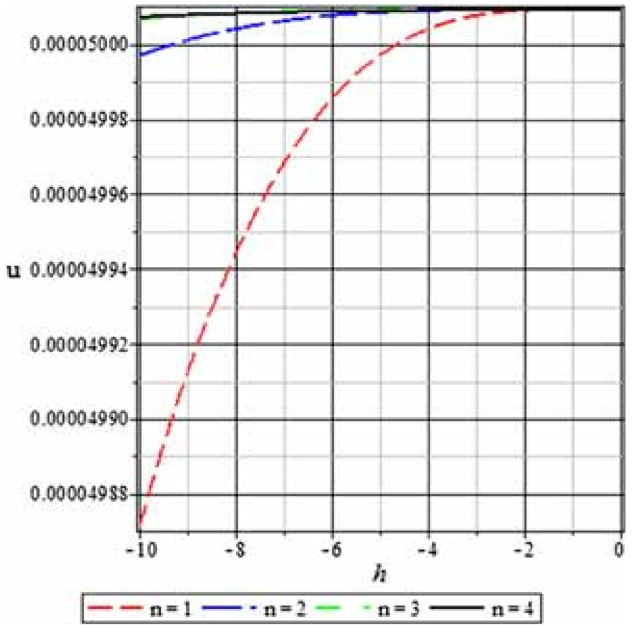

Figure 18. h-curve of q-HATM solution for different values of n at $t = 0.5$, $x = 0.1$, $y = 0.1$ and $\beta = 1$, for Example 2.

6. Basic idea of the Laplace decomposition method

In this section, we present the basic theory and solution procedure of the Laplace decomposition method. We take a general fractional nonlinear non-homogeneous partial differential equation of the form [51–54]

$$D_t^{\alpha} u(x,t) + Ru(x,t) + Nu(x,t) = g(x,t),\quad n-1 < \alpha \le n, \tag{11}$$

where $D_t^{\alpha} u(x,t)$ represents the fractional derivative of the function $u(x,t)$ in terms of Caputo, R indicates the linear differential operator, N represents the general nonlinear differential operator and $g(x,t)$ is the source term.

By applying the Laplace transform operator on both sides of eq. (11), we get

$$L\big[D_t^{\alpha} u(x,t)\big] + L[Ru(x,t)] + L[Nu(x,t)] = L[g(x,t)].$$

On using the differentiation property of the Laplace transform, it yields

$$s^{\alpha} L[u] - \sum_{k=0}^{n-1} s^{\alpha-k-1} u^{(k)}(x,0) + L[Ru] + L[Nu] = L[g(x,t)].$$

On simplification, the above equation reduces to

$$L[u(x,t)] - \frac{1}{s^{\alpha}} \sum_{k=0}^{n-1} s^{\alpha-k-1} u^{(k)}(x,0) + \frac{1}{s^{\alpha}} (L[Ru(x,t)] + L[Nu(x,t)] - L[g(x,t)]) = 0.$$

Operating inverse Laplace transform, we get

$$u(x,t) = G(x,t) - L^{-1}\big(s^{-\alpha}(L[Ru(x,t)] + L[Nu(x,t)])\big), \tag{12}$$

where $G(x,t)$ represents the term arising from the source term under the prescribed initial condition.

Next, we decompose the unknown function $u(x,t)$ into the sum of an infinite number of components given by the series

$$u(x,t) = \sum_{n=0}^{\infty} u_n(x,t) \tag{13}$$

and the nonlinear term can be decomposed as

$$Nu(x,t) = \sum_{n=0}^{\infty} A_n, \tag{14}$$

where A_n is the Adomain polynomial, given by

$$A_n = \frac{1}{(n+1)} \left[\frac{\mathrm{d}^n}{\mathrm{d}\lambda^n} \left[N \sum_{i=0}^{\infty} \lambda^i u_i(x,t) \right] \right]_{\lambda=0},$$

where $n = 0, 1, 2, 3, \ldots$.

After substituting the decomposition series (13) and (14) into eq. (12), we get

$$\sum_{n=0}^{\infty} u_n(x,t) = G(x,t) - L^{-1}\left(s^{-\alpha} \left(L\left[R \sum_{n=0}^{\infty} u_n(x,t) \right] + L\left[\sum_{n=0}^{\infty} A_n \right] \right) \right). \tag{15}$$

Equating the term on both sides of the above equation, we get the following relation:

$$u_0(x,t) = G(x,t),$$
$$u_{n+1}(x,t) = L^{-1}\big(s^{-\alpha}(L[Ru_n(x,t)] + L[A_n])\big).$$

Example 1. In the present model, we study the nonlinear time-FZK (2, 2, 2) equation [40] as

$$D_t^{\beta} u + (u^2)_x + \frac{1}{8}(u^2)_{xxx} + \frac{1}{8}(u^2)_{xyy} = 0$$

Table 4. Absolute error when $t = 1$, $\beta = 1$, $h = -1$, $n = 1$ and $\rho = 0.001$, for Example 2.

	y	x					
		0	0.02	0.04	0.06	0.08	0.10
q-HATM	0.00	2.5×10^{-7}	2.5×10^{-7}	2.5×10^{-7}	2.5×10^{-7}	2.5×10^{-7}	2.5×10^{-7}
LDM		2.5×10^{-7}	2.5×10^{-7}	2.5×10^{-7}	2.5×10^{-7}	2.5×10^{-7}	2.5×10^{-7}
VIM [28]		2.5×10^{-7}	2.5×10^{-7}	2.5×10^{-7}	2.5×10^{-7}	2.5×10^{-7}	2.5×10^{-7}
HPTM [30]		2.5×10^{-7}	2.5×10^{-7}	2.5×10^{-7}	2.5×10^{-7}	2.5×10^{-7}	2.5×10^{-7}
q-HATM	0.02	2.5×10^{-7}	2.5×10^{-7}	2.5×10^{-7}	2.5×10^{-7}	2.5×10^{-7}	2.5×10^{-7}
LDM		2.5×10^{-7}	2.5×10^{-7}	2.5×10^{-7}	2.5×10^{-7}	2.5×10^{-7}	2.5×10^{-7}
VIM [28]		2.5×10^{-7}	2.5×10^{-7}	2.5×10^{-7}	2.5×10^{-7}	2.5×10^{-7}	2.5×10^{-7}
HPTM [30]		2.5×10^{-7}	2.5×10^{-7}	2.5×10^{-7}	2.5×10^{-7}	2.5×10^{-7}	2.5×10^{-7}
q-HATM	0.04	2.5×10^{-7}	2.5×10^{-7}	2.5×10^{-7}	2.5×10^{-7}	2.5×10^{-7}	2.5×10^{-7}
LDM		2.5×10^{-7}	2.5×10^{-7}	2.5×10^{-7}	2.5×10^{-7}	2.5×10^{-7}	2.5×10^{-7}
VIM [28]		2.5×10^{-7}	2.5×10^{-7}	2.5×10^{-7}	2.5×10^{-7}	2.5×10^{-7}	2.5×10^{-7}
HPTM [30]		2.5×10^{-7}	2.5×10^{-7}	2.5×10^{-7}	2.5×10^{-7}	2.5×10^{-7}	2.5×10^{-7}
q-HATM	0.06	2.5×10^{-7}	2.5×10^{-7}	2.5×10^{-7}	2.5×10^{-7}	2.5×10^{-7}	2.5×10^{-7}
LDM		2.5×10^{-7}	2.5×10^{-7}	2.5×10^{-7}	2.5×10^{-7}	2.5×10^{-7}	2.5×10^{-7}
VIM [28]		2.5×10^{-7}	2.5×10^{-7}	2.5×10^{-7}	2.5×10^{-7}	2.5×10^{-7}	2.5×10^{-7}
HPTM [30]		2.5×10^{-7}	2.5×10^{-7}	2.5×10^{-7}	2.5×10^{-7}	2.5×10^{-7}	2.5×10^{-7}
q-HATM	0.08	2.5×10^{-7}	2.5×10^{-7}	2.5×10^{-7}	2.5×10^{-7}	2.5×10^{-7}	2.5×10^{-7}
LDM		2.5×10^{-7}	2.5×10^{-7}	2.5×10^{-7}	2.5×10^{-7}	2.5×10^{-7}	2.5×10^{-7}
VIM [28]		2.5×10^{-7}	2.5×10^{-7}	2.5×10^{-7}	2.5×10^{-7}	2.5×10^{-7}	2.5×10^{-7}
HPTM [30]		2.5×10^{-7}	2.5×10^{-7}	2.5×10^{-7}	2.5×10^{-7}	2.5×10^{-7}	2.5×10^{-7}
q-HATM	0.10	2.5×10^{-7}	2.5×10^{-7}	2.5×10^{-7}	2.5×10^{-7}	2.5×10^{-7}	2.5×10^{-7}
LDM		2.5×10^{-7}	2.5×10^{-7}	2.5×10^{-7}	2.5×10^{-7}	2.5×10^{-7}	2.5×10^{-7}
VIM [28]		2.5×10^{-7}	2.5×10^{-7}	2.5×10^{-7}	2.5×10^{-7}	2.5×10^{-7}	2.5×10^{-7}
HPTM [30]		2.5×10^{-7}	2.5×10^{-7}	2.5×10^{-7}	2.5×10^{-7}	2.5×10^{-7}	2.5×10^{-7}

Table 5. Absolute error when $t = 1$, $\beta = 1$, $h = -1.9$, $n = 2$ and $\rho = 0.001$, for Example 2.

y	x					
	0	0.02	0.04	0.06	0.08	0.1
0.00	6.26×10^{-8}	6.26×10^{-8}	6.26×10^{-8}	6.26×10^{-8}	6.26×10^{-8}	6.26×10^{-8}
0.02	6.26×10^{-8}	6.26×10^{-8}	6.26×10^{-8}	6.26×10^{-8}	6.26×10^{-8}	6.26×10^{-8}
0.04	6.26×10^{-8}	6.26×10^{-8}	6.26×10^{-8}	6.26×10^{-8}	6.26×10^{-8}	6.26×10^{-8}
0.06	6.26×10^{-8}	6.26×10^{-8}	6.26×10^{-8}	6.26×10^{-8}	6.26×10^{-8}	6.26×10^{-8}
0.08	6.26×10^{-8}	6.26×10^{-8}	6.26×10^{-8}	6.26×10^{-8}	6.26×10^{-8}	6.26×10^{-8}
0.10	6.26×10^{-8}	6.26×10^{-8}	6.26×10^{-8}	6.26×10^{-8}	6.26×10^{-8}	6.26×10^{-8}

Table 6. Absolute error when $t = 1$, $\beta = 1$, $h = -2.9$, $n = 3$ and $\rho = 0.001$, for Example 2.

y	x					
	0	0.02	0.04	0.06	0.08	0.1
0.00	2.77×10^{-8}	2.77×10^{-8}	2.77×10^{-8}	2.77×10^{-8}	2.77×10^{-8}	2.77×10^{-8}
0.02	2.77×10^{-8}	2.77×10^{-8}	2.77×10^{-8}	2.77×10^{-8}	2.77×10^{-8}	2.77×10^{-8}
0.04	2.77×10^{-8}	2.77×10^{-8}	2.77×10^{-8}	2.77×10^{-8}	2.77×10^{-8}	2.77×10^{-8}
0.06	2.77×10^{-8}	2.77×10^{-8}	2.77×10^{-8}	2.77×10^{-8}	2.77×10^{-8}	2.77×10^{-8}
0.08	2.77×10^{-8}	2.77×10^{-8}	2.77×10^{-8}	2.77×10^{-8}	2.77×10^{-8}	2.77×10^{-8}
0.10	2.77×10^{-8}	2.77×10^{-8}	2.77×10^{-8}	2.77×10^{-8}	2.77×10^{-8}	2.77×10^{-8}

Table 7. Absolute error when $t = 1, \beta = 1, h = -99.9, n = 100$ and $\rho = 0.001$, for Example 2.

y	x					
	0	0.02	0.04	0.06	0.08	0.1
0.00	2.5×10^{-11}	2.5×10^{-11}	2.5×10^{-11}	2.5×10^{-11}	2.5×10^{-11}	2.5×10^{-11}
0.02	2.5×10^{-11}	2.5×10^{-11}	2.5×10^{-11}	2.5×10^{-11}	2.5×10^{-11}	2.5×10^{-11}
0.04	2.5×10^{-11}	2.5×10^{-11}	2.5×10^{-11}	2.5×10^{-11}	2.5×10^{-11}	2.5×10^{-11}
0.06	2.5×10^{-11}	2.5×10^{-11}	2.5×10^{-11}	2.5×10^{-11}	2.5×10^{-11}	2.5×10^{-11}
0.08	2.5×10^{-11}	2.5×10^{-11}	2.5×10^{-11}	2.5×10^{-11}	2.5×10^{-11}	2.5×10^{-11}
0.10	2.5×10^{-11}	2.5×10^{-11}	2.5×10^{-11}	2.5×10^{-11}	2.5×10^{-11}	2.5×10^{-11}

Table 8. Absolute error when $t = 1, \beta = 1, h = -999.9, n = 1000$ and $\rho = 0.001$, for Example 2.

y	x					
	0	0.02	0.04	0.06	0.08	0.1
0.00	2.1×10^{-13}	2.1×10^{-13}	2.1×10^{-13}	2.1×10^{-13}	2.1×10^{-13}	2.1×10^{-13}
0.02	2.1×10^{-13}	2.1×10^{-13}	2.1×10^{-13}	2.1×10^{-13}	2.1×10^{-13}	2.1×10^{-13}
0.04	2.1×10^{-13}	2.1×10^{-13}	2.1×10^{-13}	2.1×10^{-13}	2.1×10^{-13}	2.1×10^{-13}
0.06	2.1×10^{-13}	2.1×10^{-13}	2.1×10^{-13}	2.1×10^{-13}	2.1×10^{-13}	2.1×10^{-13}
0.08	2.1×10^{-13}	2.1×10^{-13}	2.1×10^{-13}	2.1×10^{-13}	2.1×10^{-13}	2.1×10^{-13}
0.10	2.1×10^{-13}	2.1×10^{-13}	2.1×10^{-13}	2.1×10^{-13}	2.1×10^{-13}	2.1×10^{-13}

subject to the initial condition

$$u(x, y, 0) = \frac{4}{3}\rho \sinh^2(x + y),$$

where ρ is an arbitrary constant.

On applying the LDM to solve the above equations, we get the following successive approximations:

$$u_0(x, y, t) = \frac{4}{3}\rho \sinh^2(x + y),$$

$$u_1(x, y, t) = -\left[\frac{224}{9}\rho^2 \sinh^3(x + y)\cosh(x + y) + \frac{32}{3}\rho^2 \sinh(x + y)\cosh^3(x + y)\right]\frac{t^{\beta}}{\Gamma(\beta + 1)},$$

$$u_2(x, y, t) = \frac{64}{27}\rho^3[2400\cosh^6(x + y) - 4160\cosh^4(x + y) + 1936\cosh^2(x + y) - 158]\frac{t^{2\beta}}{\Gamma(2\beta + 1)},$$

$$u_3(x, y, t) = -\rho^4\frac{256}{9}\{403200\sinh^3(x + y) \times \cosh^5(x + y) + 144000\sinh^5(x + y)\cosh^3(x + y) + 105600\sinh(x + y)\cosh^7(x + y) - 49920\sinh^5(x + y)\cosh(x + y) - 133120\sinh(x + y)\cosh^5(x + y) - 316160\sinh^3(x + y)\cosh^3(x + y) + 38716\sinh^3(x + y)\cosh(x + y) + 38716\sinh(x + y)\cosh^3(x + y) - 1264\sinh(x + y)\cosh(x + y)\}\frac{t^{3\beta}}{\Gamma(3\beta + 1)}$$

$$-\rho^4\left\{\frac{50176}{81}[30\sinh^3(x + y)\cosh^5(x + y) + 84\sinh^5(x + y)\cosh^3(x + y) + 22\sinh^7(x + y)\cosh(x + y)] + \frac{1024}{9}[22\sinh(x + y)\cosh^7(x + y)\right.$$

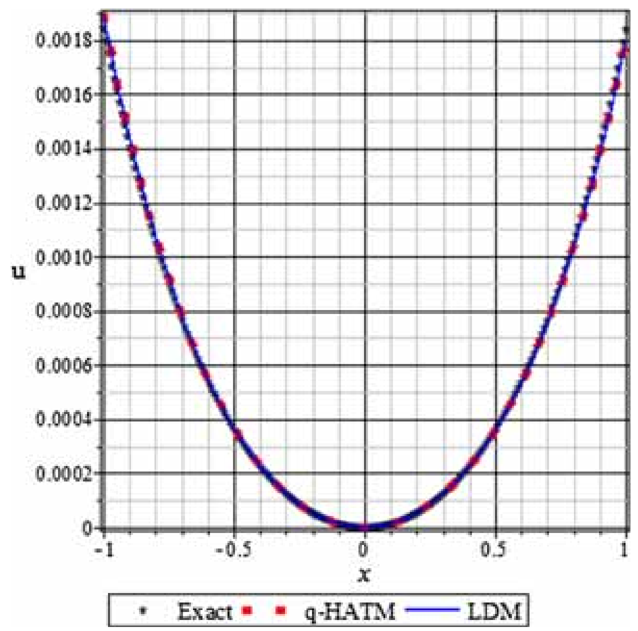

Figure 19. Comparison of exact, q-HATM and LDM solutions when $t = 0.5, n = 1, h = -1, y = 0, \rho = 0.001$ and $\beta = 1$, for Example 1.

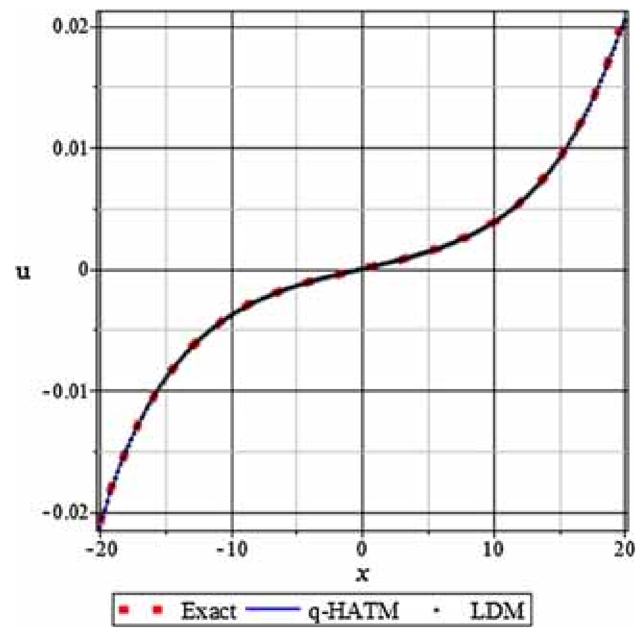

Figure 20. Comparison of exact, q-HATM and LDM solutions when $t = 0.5, n = 1, h = -1, y = 0, \rho = 0.001$ and $\beta = 1$, for Example 2.

$$+ 84 \sinh^3(x+y)\cosh^5(x+y)$$
$$+ 20 \sinh^5(x+y)\cosh^3(x+y)]$$
$$+ \frac{14336}{27}[6\sinh(x+y)\cosh^7(x+y)$$
$$+ 6\sinh^7(x+y)\cosh(x+y)$$
$$+ 52\sinh^5(x+y)\cosh^3(x+y)$$
$$+ 52\sinh^3(x+y)\cosh^5(x+y)]\Big\}$$
$$\times \frac{\Gamma(2\beta+1)t^{3\beta}}{(\Gamma(\beta+1))^2\Gamma(3\beta+1)}.$$

In the same manner, the rest of the components of the LDM solution can be obtained. We observed that the LDM solution can be obtained as a special case of the q-HATM solution just by putting $h = -1$ and $n = -1$ (see figure 19).

Example 2. In the present model, we study the nonlinear time-FZK (3, 3, 3) equation [40] as

$$D_t^\beta u + (u^3)_x + 2(u^3)_{xxx} + 2(u^3)_{xyy} = 0, \quad 0 < \beta \le 1$$

subject to the initial condition

$$u(x, y, 0) = \frac{3}{2}\rho \sinh\left(\frac{1}{6}(x+y)\right),$$

where ρ is an arbitrary constant.

Applying the LDM to solve the above equations, we get the following successive approximations:

$$u_0(x, y, t)$$
$$= \frac{3}{2}\rho \sinh\left[\frac{1}{6}(x+y)\right],$$
$$u_1(x, y, t)$$
$$= -3\rho^3\left[\sinh^3\frac{1}{6}(x+y)\right]\cosh\left[\frac{1}{6}(x+y)\right]$$
$$+ \frac{1}{8}\cosh^3\left[\frac{1}{6}(x+y)\right]\frac{t^\beta}{\Gamma(\beta+1)},$$
$$u_2(x, y, t)$$
$$= \frac{3}{64}\rho^5 \sinh\left[\frac{1}{6}(x+y)\right]\left\{1530\cosh^4\left[\frac{1}{6}(x+y)\right]\right.$$
$$\left. - 1458\cosh^2\left[\frac{1}{6}(x+y) + 182\right]\right\}\frac{t^{2\beta}}{\Gamma(2\beta+1)},$$
$$u_3(x, y, t)$$
$$= -\frac{27}{1536}\rho^7\left\{3060\cosh^7\left[\frac{1}{6}(x+y)\right]\right.$$
$$+ 79560\cosh^5\left[\frac{1}{6}(x+y)\right]$$
$$\times \sinh^2\left[\frac{1}{6}(x+y)\right] + 112200\cosh^3\left[\frac{1}{6}(x+y)\right]$$

$$\times\sinh^4\left[\frac{1}{6}(x+y)\right]$$
$$+12240\cosh\left[\frac{1}{6}(x+y)\right]\sinh^6\left[\frac{1}{6}(x+y)\right]$$
$$-30132\cosh\left[\frac{1}{6}(x+y)\right]\sinh^4\left[\frac{1}{6}(x+y)\right]$$
$$-49572\cosh^3\left[\frac{1}{6}(x+y)\right]\sinh^2\left[\frac{1}{6}(x+y)\right]$$
$$-2916\cosh^5\left[\frac{1}{6}(x+y)\right]$$
$$+2915\cosh\left[\frac{1}{6}(x+y)\right]\sinh^2\left[\frac{1}{6}(x+y)\right]$$
$$+364\cosh^3\left[\frac{1}{6}(x+y)\right]\Bigg\}\frac{t^{3\beta}}{\Gamma(3\beta+1)}$$
$$-\frac{27}{12}\rho^5\Bigg\{70\cosh^5\left[\frac{1}{6}(x+y)\right]\sinh^4\left[\frac{1}{6}(x+y)\right]$$
$$+\frac{490}{3}\cosh^3\left[\frac{1}{6}(x+y)\right]\sinh^6\left[\frac{1}{6}(x+y)\right]$$
$$+\frac{110}{3}\cosh\left[\frac{1}{6}(x+y)\right]\sinh^8\left[\frac{1}{6}(x+y)\right]$$
$$+\frac{84}{64}\cosh^5\left[\frac{1}{6}(x+y)\sinh^2\left[\frac{1}{6}(x+y)\right]\right.$$
$$+\frac{28}{192}\cosh^7\left[\frac{1}{6}(x+y)\right]$$
$$+\frac{40}{64}\cosh^3\left[\frac{1}{6}(x+y)\right]\sinh^4\left[\frac{1}{6}(x+y)\right]$$
$$+2\cosh^6\left[\frac{1}{6}(x+y)\right]\sinh\left[\frac{1}{6}(x+y)\right]$$
$$+\frac{67}{3}\cosh^5\left[\frac{1}{6}(x+y)\right]\sinh^3\left[\frac{1}{6}(x+y)\right]$$
$$+\frac{67}{3}\cosh^3\left[\frac{1}{6}(x+y)\right]\sinh^5\left[\frac{1}{6}(x+y)\right]$$
$$+2\cosh\left[\frac{1}{6}(x+y)\right]\sinh^7\left[\frac{1}{6}(x+y)\right]\Bigg\}$$
$$\times\frac{\Gamma(2\beta+1)t^{3\beta}}{\Gamma(3\beta+1)(\Gamma(\beta+1))^2}.$$

In the same manner, the rest of the components of the LDM solution can be obtained. We observed that the LDM solution can be obtained as a special case of q-HATM solution just by putting $h=-1$ and $n=-1$ (see figure 20).

7. Conclusions

In this paper, we implemented q-HATM and LDM to find the solution of nonlinear time-FZK equations. We obtained the solution of nonlinear models in the form of a convergent series by q-HATM without any type of conventions. If we take $n=1$ and $h=-1$ in the q-HATM solution, we have the solution as obtained by using LDM, HPM and VIM. So LDM, HPM and VIM are special cases of q-HATM under these conditions. The fact that the q-HATM solves nonlinear models without using Adomian's polynomials is a clear advantage of this technique over the decomposition method. Hence, we conclude that the present scheme is reliable and powerful in finding numerical solutions for wide classes of nonlinear fractional partial differential equations.

Acknowledgements

The authors are thankful to the anonymous reviewers and editors for their valuable comments and suggestions to improve the quality of this paper.

References

[1] J H He, *Commun. Nonlinear Sci. Numer. Simul.* **2**, 235 (1997)
[2] J H He, *Commun. Nonlinear Sci. Numer. Simul.* **3**, 92 (1998)
[3] A Prakash, M Kumar and K K Sharma, *Appl. Math. Comput.* **260**, 314 (2015)
[4] A Prakash and M Kumar, *J. Appl. Anal. Comput.* **6**(**3**), 738 (2016)
[5] A Prakash and M Kumar, *Open Phys.* **14**, 177 (2016)
[6] A Yildirim, *Int. J. Nonlinear Sci. Numer. Simul.* **10**(**4**), 445 (2009)
[7] A Yildirim, *J. King Saud Univ. (Sci.)* **22**, 257 (2010)
[8] S J Liao, *Appl. Math. Comput.* **147**, 499 (2004)
[9] S Kumar, H Kocak and A Yildirim, *Z. Naturforsch. A* **67**, 389 (2012)
[10] S Kumar, A Yildirim, Y Khan and L Wei, *Sci. Iran B* **19**(**4**), 1117 (2012)
[11] D Kumar, J Singh and D Baleanu, *J. Comput. Nonlinear Dyn.* **11**(**6**), 061004 (2016)
[12] A Prakash, M Kumar and D Baleanu, *Appl. Math. Comput.* **334**, 30 (2018)
[13] H M Baskonus and H Bulut, *Open Math.* **13**(**1**), 547 (2015)
[14] D G Prakasha, P Veeresha and H M Baskonus, *Fractal Fract.* **3**(**9**), 1 (2019)

[15] D G Prakasha, P Veeresha and H M Baskonus, *Comput. Math. Methods* **1(2)**, 1 (2019)
[16] M Arshad, Aly Seadawy, Dianchen Lu and Jem Wang, *Results Phys.* **6**, 1136 (2016)
[17] J Singh, D Kumar and D Baleanu, *Math. Model. Nat. Phenom.* **14**, 303 (2019)
[18] P Veeresha, D G Prakasha and H M Baskonus, *Math. Sci.* (2019), https://doi.org/10.1007/s40096-019-0284-6
[19] P Veeresha, D G Prakasha and H M Baskonus, *AIP Chaos Interdiscip. J. Nonlinear Sci.* **29**(**1**), 1 (2019)
[20] M T Gencoglu, H M Baskonus and H Bulut, *AIP Conf. Proc.* **1798**, 1 (2017)
[21] M Goyal, A Prakash and S Gupta, *Pramana – J. Phys.* **92**: 82 (2019)
[22] A Prakash, M Goyal and S Gupta, *Pramana – J. Phys.* **92**(**2**): 1 (2019)
[23] M A El-Tawil and S N Huseen, *Int. J. Appl. Math. Mech.* **8**, 51 (2012)
[24] M A El-Tawil and S N Huseen, *Int. J. Contemp. Math. Sci.* **8**, 481 (2013)
[25] S J Liao, *The proposed homotopy analysis technique for the solution of nonlinear problems*, Ph.D. thesis (Shanghai Jiao Tong Univ., 1992)
[26] S J Liao, *Commun. Nonlinear Sci. Numer. Simul.* **2**, 95 (1997)
[27] S J Liao, *Beyond perturbation: Introduction to the homotopy analysis method* (Chapman and Hall/CRC Press, Boca Raton, 2003)
[28] D L Xu, Z L Lin, S J Liao and M Stiassnie, *J. Fluid Mech.* **710**, 379 (2012)
[29] S J Liao, *Math. Comput.* **147**, 499 (2004)
[30] H Jafari, A Golbabai, S Seifi and K Sayevand, *Comput. Math. Appl.* **66**, 838 (2010)
[31] S Kumar, A Kumar and D Baleanu, *Nonlinear Dyn.* **85**(**2**), 699 (2016), https://doi.org/10.1007/s11071-016-2716-2
[32] S Nadeem, A Hussain and M Khan, *Z. Naturforsch.* **65**, 540 (2010)
[33] M Khan, M A Gondal, I Hussain and S Karimi Vanani, *Math. Comput. Model.* **55**, 1143 (2012)
[34] D Kumar, J Singh and Sushila, *Rom. Rep. Phys.* **65**(**1**), 63 (2013)
[35] D Kumar, J Singh, S Kumar and Sushila, *Alex. Eng. J.* **53**(**2**), 469 (2014)
[36] S Munro and E J Parkes, *J. Plasma Phys.* **62**(**3**), 305 (1999)
[37] S Munro and E J Parkes, *J. Plasma Phys.* **64**(**4**), 411 (2000)
[38] V E Sakharov and E A Kuznetsov, *Sov. Phys. JETP* **39**, 285 (1974)
[39] R Y Molliq, M S M Noorani, I Hashim and R R Ahmad, *J. Comput. Appl. Math.* **233**, 103 (2009)
[40] A Yildirim and Y Gulkanat, *Commun. Theor. Phys.* **53**, 1005 (2010)
[41] D Kumar, J Singh and S Kumar, *J. Egypt. Math. Soc.* **22**, 373 (2014)
[42] D Kumar, J Singh and D Baleanu, *Nonlinear Dyn.* **87**(**1**), 511 (2019). https://doi.org/10.1007/s11071-016-3057-x
[43] X J Yang, J A T Machado and J Haristov, *Nonlinear Dyn.* **84**, 3 (2016)
[44] E H Doha, A H Bhrawy and S S Ezz-Eldien, *J. Comput. Nonlinear Dyn.* **10**, 1 (2015)
[45] I Podlubny, *Fractional differential equations* (Academic Press, New York, 1999)
[46] M Inc, *Chaos Solitons Fractals* **33**(**5**), 1783 (2007)
[47] P Veeresha, D G Prakasha and D Baleanu, *Mathematics* **7**, 265 (2019)
[48] I K Argyros, *Convergence and applications of Newton-type iterations* (Springer Science and Business Media, Berlin, Germany, 2008)
[49] A A Magrenam, *Appl. Math. Comput.* **248**, 215 (2014)
[50] Z M Odibat and N T Shawagfeh, *Appl. Math. Comput.* **186**, 286 (2007)
[51] H Jafari, C M Khalique and M Nazari, *Appl. Math. Lett.* **24**, 1799 (2011)
[52] H M Srivastava, D Kumar and J Singh, *Appl. Math. Model.* **45**, 192 (2017)
[53] A M Wazwaz and M S Mehana, *Nonlinear Sci.* **10**, 248 (2010)
[54] M Khan and M Hussain, *Numer. Algorithms* **56**, 211 (2011)